



# THE UNIVERSITY *of* EDINBURGH

## Edinburgh Research Explorer

### Realistic Source Modeling in Wave-based Virtual Acoustics

**Citation for published version:**

Bilbao, S 2021, Realistic Source Modeling in Wave-based Virtual Acoustics. in *Forum Acusticum*. HAL, Lyon, France, pp. 533-539. <<https://hal.archives-ouvertes.fr/FA2020/hal-03235238>>

**Link:**

[Link to publication record in Edinburgh Research Explorer](#)

**Document Version:**

Publisher's PDF, also known as Version of record

**Published In:**

Forum Acusticum

**General rights**

Copyright for the publications made accessible via the Edinburgh Research Explorer is retained by the author(s) and / or other copyright owners and it is a condition of accessing these publications that users recognise and abide by the legal requirements associated with these rights.

**Take down policy**

The University of Edinburgh has made every reasonable effort to ensure that Edinburgh Research Explorer content complies with UK legislation. If you believe that the public display of this file breaches copyright please contact [openaccess@ed.ac.uk](mailto:openaccess@ed.ac.uk) providing details, and we will remove access to the work immediately and investigate your claim.



# REALISTIC SOURCE MODELING IN WAVE-BASED VIRTUAL ACOUSTICS

Stefan Bilbao<sup>1</sup>

<sup>1</sup> Acoustics and Audio Group, University of Edinburgh, United Kingdom

sbilbao@ed.ac.uk

## ABSTRACT

The modelling of sources in wave-based virtual acoustics has a long history, and many forms have emerged, including hard, soft and transparent sources. What has been lacking is an underlying model against which numerically-computed solutions may be compared. In this paper, a fully spatio-temporal 1D source model is presented, framed in terms of a source impedance, source strength and employing localised distributions (Dirac delta functions) and their distributional derivatives as additional driving terms in the wave equation; such a model allows for the interaction of the source with the field, through both the generation of wave energy and reflection of incoming waves. Exact solutions may be deduced for the model, and the model itself is fully general and independent of any particular discretisation technique. As the model incorporates feedback, new concerns regarding numerical stability for any resulting numerical method emerge, but can be handled using energy balance techniques. Numerical simulation results are presented.

## 1. INTRODUCTION

Source modeling in volumetric wave-based acoustic simulation methods (such as, e.g., the finite difference time domain method [1–4] or FDTD) can be traced back to Schneider et al. [5]. Various approaches are described in [6–8]. These include the “hard source,” in which case a pressure value at a given grid point is fixed to an external input signal value, the “soft source,” in which case the external input signal is added into the simulation, and approaches designed to reduce artefacts, including the “transparent source” model. All of the source excitation frameworks mentioned above employ a numerical method as a starting point; they describe different strategies for injecting a discrete time source signal into a simulation. What is lacking is an underlying model, posed as a continuous-time/space PDE system. Without such a model at hand, it is difficult to compare the merits of two different excitation strategies, as they may be solving entirely different problems.

Typical continuous source models which appear in the literature are framed in terms of the wave equation accompanied by an additive excitation term (often separated into a product of a spatial distribution, sometimes idealised to

a Dirac distribution, with a time-dependent source excitation function). See, e.g., [9]. Such models have been used recently in the emulation of sources of arbitrary directivity in an FDTD setting [10]. Such sources correspond to numerical excitations of soft or additive type mentioned above—the source itself does not reflect incoming waves. This is obviously not the case in practice—the source behaves as a boundary as well as a means of injecting energy, as in the case of the hard source model, and some immittance model of the source behaviour itself is necessary. Source modeling with an immittance has been described in [11], though without reference to an underlying model. This paper is concerned with the presentation of a general PDE model of sources including such reflective behaviour, and approaches to numerical design, and may be classified as an immersed boundary method [12–14]. As such a model includes feedback mechanisms, allowing for an energy storage mechanism in the source itself, new concerns appear in terms of numerical stability, and will be investigated here.

In Section 2, a general model for a point-like source is presented in the simplified setting of 1D acoustics; such a model is characterised by two immittances, and is capable of both exciting the acoustic field and reflecting incoming waves. It contains so-called hard and soft source behaviour as special cases, and allows for monopole- and dipole excitation. A semi-discrete model is presented in Section 3, followed by a fully discrete model in Section 4. Simulation results appear in Section 5.

## 2. MODEL

Consider the following model of a source in a 1D acoustic setting:

$$\rho \partial_t v + \partial_x p = p_\Delta \delta(x) \quad \frac{1}{\rho c^2} \partial_t p + \partial_x v = v_\Delta \delta(x) \quad (1)$$

Here,  $p(x, t)$  and  $v(x, t)$  represent acoustic pressure and particle velocity, respectively, as a function of coordinate  $x \in \mathbb{R}$  and for time  $t \geq 0$ .  $\partial_x$  and  $\partial_t$  represent differentiation with respect to  $x$  and  $t$ .  $\rho$  is the density of air in  $\text{kg}\cdot\text{m}^{-3}$  and  $c$  is wave speed, in  $\text{m}\cdot\text{s}^{-1}$ . System (1) is completed by two initial distributions:

$$v(x, 0) = v_0(x) \quad p(x, 0) = p_0(x)$$

The source terms are activated by Dirac delta functions  $\delta$  located, without loss of generality, at  $x = 0$ , and of corresponding strengths  $v_\Delta = v_\Delta(t)$  and  $p_\Delta = p_\Delta(t)$ . In most cases, these are considered to be external driving functions; here we do not make that assumption. We will return to the forms of  $v_\Delta$  and  $p_\Delta$  which are coupled to the acoustic field in Section 2.1. Here we employ pure point sources, but the model above (and the development to follow) is altered only slightly if a finite-width distribution is used instead of the Dirac delta.

A second order form follows immediately as

$$\frac{1}{c^2} \partial_t^2 p - \partial_x^2 p = \rho \dot{v}_\Delta \delta(x) - p_\Delta \delta'(x)$$

where dots and primes indicate ordinary temporal and spatial differentiation.

## 2.1 Coupling to the Acoustic Field

Consider the following model:

$$p_\Delta = p_d - p_c \quad v_\Delta = v_m - v_c \quad (2)$$

Here,  $v_m(t)$  and  $p_d(t)$  are externally supplied excitation functions, assumed zero for  $t < 0$ . The terms  $p_c$  and  $v_c$  are derived from the acoustic field at the excitation location  $x = 0$  by the differential relationships

$$\sum_{\nu=0}^{D_d} \zeta_{d,\nu} (d/dt)^\nu p_c = Z_0 \sum_{\nu=0}^{M_d} \eta_{d,\nu} \partial_t^\nu v|_{x=0} \quad (3a)$$

$$\sum_{\nu=0}^{D_m} \zeta_{m,\nu} (d/dt)^\nu v_c = Y_0 \sum_{\nu=0}^{M_m} \eta_{m,\nu} \partial_t^\nu p|_{x=0} \quad (3b)$$

defined in terms of the constants  $\eta_{d,\nu}$ ,  $\zeta_{d,\nu}$ ,  $\eta_{m,\nu}$  and  $\zeta_{m,\nu}$ , and for specified orders  $M_d$ ,  $D_d$ ,  $M_m$  and  $D_m$ . The constants will be constrained, shortly, so that the relationships (3) above correspond, in the frequency domain, to passive immittances.  $Z_0 = \rho c$  is the characteristic impedance of air, and  $Y_0 = 1/Z_0$  is the characteristic admittance. For simplicity here, the functions  $p_c$  and  $v_c$ , as well as the acoustic field at  $x = 0$  are assumed quiescent at  $t = 0$ , so that additional initial conditions need not be taken into account in the eventual resolution of (3).

## 2.2 Laplace Transformation

A solution to (1), under one-sided Laplace transformation from time  $t$  to a complex frequency variable  $s$  may be derived as

$$\hat{v}(x, s) = \hat{v}_F(x, s) + \hat{v}_S(x, s) \quad (4a)$$

$$\hat{p}(x, s) = \hat{p}_F(x, s) + \hat{p}_S(x, s) \quad (4b)$$

where

$$\hat{v}_F = \frac{1}{2c} \int_{-\infty}^{\infty} (v_0(\xi) + Y_0 p_0(\xi) \operatorname{sgn}(x - \xi)) e^{-\frac{s|x-\xi|}{c}} d\xi$$

$$\hat{v}_S = \frac{1}{2} (\hat{v}_\Delta \operatorname{sgn}(x) + Y_0 \hat{p}_\Delta) e^{-\frac{s}{c}|x|}$$

$$\hat{p}_F = \frac{1}{2c} \int_{-\infty}^{\infty} (p_0(\xi) + Z_0 v_0(\xi) \operatorname{sgn}(x - \xi)) e^{-\frac{s|x-\xi|}{c}} d\xi$$

$$\hat{p}_S = \frac{1}{2} (\hat{p}_\Delta \operatorname{sgn}(x) + Z_0 \hat{v}_\Delta) e^{-\frac{s}{c}|x|}$$

Here,  $\hat{v}(x, s)$  and  $\hat{p}(x, s)$  are the Laplace transforms of  $v$  and  $p$ , respectively (and similarly for  $\hat{v}_\Delta(s)$  and  $\hat{p}_\Delta(s)$ ).  $\operatorname{sgn}(\cdot)$  is the signum function. For externally-supplied source signals  $v_\Delta$  and  $p_\Delta$ , the solution (4) is complete, and consists of a sum of traveling wave terms ( $\hat{v}_F$ ,  $\hat{p}_F$ ) and excitation terms ( $\hat{v}_S$ ,  $\hat{p}_S$ ). In particular, the source does not interact with the acoustic field other than as a driving term.

Now introduce the Laplace transform of the coupling relationship (2):

$$\hat{p}_\Delta = \hat{p}_d - \hat{p}_c \quad \hat{v}_\Delta = \hat{v}_m - \hat{v}_c \quad (6)$$

Here,  $\hat{p}_d(s)$  and  $\hat{v}_m(s)$  are Laplace-transformed external excitation functions. The functions  $\hat{p}_c$  and  $\hat{v}_c$  are coupled into the acoustic field at the excitation location through

$$\hat{p}_c = Z_0 z_d \hat{v}(0, s) \quad \hat{v}_c = Y_0 y_m \hat{p}(0, s) \quad (7)$$

Here  $y_m(s)$  and  $z_d(s)$  are a normalized admittance and impedance, respectively, given, from (3), by

$$z_d(s) = \frac{\sum_{\nu=0}^{M_d} \eta_{d,\nu} s^\nu}{\sum_{\nu=0}^{D_d} \zeta_{d,\nu} s^\nu} \quad y_m(s) = \frac{\sum_{\nu=0}^{M_m} \eta_{m,\nu} s^\nu}{\sum_{\nu=0}^{D_m} \zeta_{m,\nu} s^\nu}$$

Both are constrained to be positive real (passive) functions of  $s$  [15, 16]. For example, for  $y_m(s)$ , we require that

$$\operatorname{Re}(y_m) \geq 0 \quad \text{when} \quad \operatorname{Re}(s) > 0 \quad (8)$$

and similarly for  $z_d$ . Note that the positive realness condition on these immittances places various restrictions on the particular form of these rational functions [15].

## 2.3 Complete Solution

From the general form of the solution in (4), evaluated at  $x = 0$ , and noting that

$$\hat{v}_S(0, s) = \frac{Y_0 \hat{p}_\Delta}{2} \quad \hat{p}_S(0, s) = \frac{Z_0 \hat{v}_\Delta}{2}$$

one obtains

$$\hat{p}_\Delta = \frac{2}{2 + z_d} (\hat{p}_d - Z_0 z_d \hat{v}_F(0, s))$$

$$\hat{v}_\Delta = \frac{2}{2 + y_m} (\hat{v}_m - Y_0 y_m \hat{p}_F(0, s))$$

the solution (4) may then be rewritten as

$$\hat{v}(x, s) = \hat{v}_F(x, s) + \hat{v}_E(x, s) + \hat{v}_R(x, s) \quad (9a)$$

$$\hat{p}(x, s) = \hat{p}_F(x, s) + \hat{p}_E(x, s) + \hat{p}_R(x, s) \quad (9b)$$

where  $\hat{v}_F$  and  $\hat{p}_F$  are as before, and where

$$\hat{v}_E = \left( \frac{\hat{v}_m}{2 + y_m} \operatorname{sgn}(x) + \frac{Y_0 \hat{p}_d}{2 + z_d} \right) e^{-\frac{s}{c}|x|}$$

$$\hat{p}_E = \left( \frac{\hat{p}_d}{2 + z_d} \operatorname{sgn}(x) + \frac{Z_0 \hat{v}_m}{2 + y_m} \right) e^{-\frac{s}{c}|x|}$$

and

$$\hat{v}_R = - \left( \frac{Y_0 y_m \hat{p}_F(0, s)}{2 + y_m} \operatorname{sgn}(x) + \frac{z_d \hat{v}_F(0, s)}{2 + z_d} \right) e^{-\frac{s}{c}|x|}$$

$$\hat{p}_R = - \left( \frac{Z_0 z_d \hat{v}_F(0, s)}{2 + z_d} \operatorname{sgn}(x) + \frac{y_m \hat{p}_F(0, s)}{2 + y_m} \right) e^{-\frac{s}{c}|x|}$$

Here,  $\hat{v}_E$  and  $\hat{p}_E$  represent the part of the solution due purely to external driving terms—note that they are affected by the source immittances. In their absence, a component of the solution due to reflections from the source location persists, through  $\hat{v}_R$  and  $\hat{p}_R$ .

## 2.4 Special Case: Zero Initial Conditions

The simplest case arises when initial conditions are zero, or that  $p_0 = v_0 = 0$ . Then,  $\hat{p} = \hat{p}_E$  and  $\hat{v} = \hat{v}_E$ . As an example, consider the very basic case of  $y_m = z_d = \text{const}$ . One arrives at (for pressure), after inverse Laplace transformation,

$$p(x, t) = \frac{p_d(t - |x|/c) \text{sgn}(x) + Z_0 v_m(t - |x|/c)}{2 + z_d} + \frac{Z_0 v_m(t - |x|/c)}{2 + y_m}$$

and we thus see a combination of basic monopole and dipole sources at  $x = 0$ .

## 3. SEMI-DISCRETE FORM

As a step towards discretisation, consider problem (1) defined over an interval of length  $L$ . The solution will be defined over two grids (interleaved) with spacing  $h$  such that  $N = L/h$  is an integer. Velocity values  $v_l(t)$  are defined for  $l = 1, \dots, N-1$  and pressure values  $p_{l+1/2}(t)$  for  $l = 0, \dots, N-1$ . Such grid functions may be consolidated into column vectors  $\mathbf{v}(t)$  and  $\mathbf{p}(t)$  as

$$\mathbf{v} = [v_1, \dots, v_{N-1}]^T \quad \mathbf{p} = [p_{1/2}, \dots, p_{N-1/2}]^T$$

A semi-discrete approximation to (1) may be written as

$$\rho \dot{\mathbf{v}} + \frac{1}{h} \mathbf{D}_- \mathbf{p} = \frac{1}{h} p_\Delta \mathbf{J}_v \quad (10a)$$

$$\frac{1}{\rho c^2} \dot{\mathbf{p}} + \frac{1}{h} \mathbf{D}_+ \mathbf{v} = \frac{1}{h} v_\Delta \mathbf{J}_p \quad (10b)$$

Here,  $(1/h)\mathbf{D}_+$  is an  $N \times (N-1)$  matrix that is an approximation to  $\partial_x$ ; assuming zero velocity conditions at the ends of the domain, and using a basic nearest neighbour finite difference approximation leads to

$$\mathbf{D}_+ = \begin{bmatrix} 1 & & & & \\ -1 & 1 & & & \\ & & \ddots & \ddots & \\ & & & -1 & 1 \\ & & & & -1 \end{bmatrix} \quad (11)$$

Here, zero velocity conditions are chosen at the domain endpoints, leading to  $\mathbf{D}_- = -\mathbf{D}_+^T$ .

$(1/h)\mathbf{J}_p$  and  $(1/h)\mathbf{J}_v$  are  $N \times 1$  and  $(N-1) \times 1$  approximations to the Dirac delta function over interleaved grids [17]. In the simplest case, these vectors could contain a single non-zero value (of 1, or a Kronecker delta function), selecting the source location, but more accurate approximation to the Delta function are available [18].

The vectors  $\mathbf{p}$  and  $\mathbf{v}$  take on initial values  $\mathbf{p}(0) = \mathbf{p}_0$  and  $\mathbf{v}(0) = \mathbf{v}_0$ , which could be sampled from the continuous initial conditions described in Section 2.

## 3.1 Laplace Transformation

Under one-sided Laplace transformation, one may define vectors  $\hat{\mathbf{p}}(s)$  and  $\hat{\mathbf{v}}(s)$ . The coupling conditions (6) may be rewritten in semidiscrete form as

$$\hat{p}_\Delta = \hat{p}_d - \hat{p}_c \quad \hat{v}_\Delta = \hat{v}_m - \hat{v}_c \quad (12)$$

where, in analogy with (7),

$$\hat{p}_c = Z_0 z_d \mathbf{J}_v^T \hat{\mathbf{v}} \quad \hat{v}_c = Y_0 y_m \mathbf{J}_p^T \hat{\mathbf{p}} \quad (13)$$

Combining the Laplace transform of the ODE system (10) with (12) and (13) leads to the complete Laplace-transformed system

$$\mathbf{A}(s) \mathbf{x}(s) = \mathbf{b}(s) \quad (14)$$

where

$$\mathbf{x} = \begin{bmatrix} \hat{\mathbf{v}} \\ \hat{\mathbf{p}} \end{bmatrix} \quad \mathbf{b} = \begin{bmatrix} \rho \mathbf{v}_0 + \frac{1}{h} \hat{p}_d \mathbf{J}_v \\ \frac{1}{\rho c^2} \mathbf{p}_0 + \frac{1}{h} \hat{v}_m \mathbf{J}_p \end{bmatrix} \quad (15)$$

and

$$\mathbf{A}(s) = \begin{bmatrix} \rho s \mathbf{I}_v + \frac{Z_0 z_d}{h} \mathbf{J}_v \mathbf{J}_v^T & -\frac{1}{h} \mathbf{D}_+ \\ \frac{1}{h} \mathbf{D}_+^T & \frac{s}{\rho c^2} \mathbf{I}_p + \frac{Y_0 y_m}{h} \mathbf{J}_p \mathbf{J}_p^T \end{bmatrix} \quad (16)$$

where  $\mathbf{I}_v$  and  $\mathbf{I}_p$  are  $(N-1) \times (N-1)$  and  $N \times N$  identity matrices, respectively.

The natural frequencies of the semi-discrete system are determined by the values of  $s$  for which the determinant of  $\mathbf{A}(s)$  vanishes. In order that the system not exhibit exponential growth, no such zeros can occur for values of  $s$  with  $\text{Re}(s) > 0$ . Following an analysis identical to that presented in [19], but now in the case of sources, rather than impedance boundary conditions, it can be shown that given the positive realness condition on the immittances in (8), no such zeros can occur. This analysis hinges here on the skew-symmetry of  $\mathbf{D}_+$  and  $\mathbf{D}_-$ , and also the use of the representations  $\mathbf{J}_p$  and  $\mathbf{J}_v$  alongside their adjoints, but is otherwise insensitive to the precise definitions of these forms. This implies a great deal of latitude in terms of the difference approximations and delta function approximations employed.

## 4. FDTD METHODS

Consider a vector time series  $\mathbf{w}^n$ , representing an approximation to some underlying continuously variable function  $\mathbf{w}(t)$  at time  $t = nk$ , for an integer index  $n$  and a time step  $k$ . Difference operators approximating a time derivative may be defined as

$$\delta_+ \mathbf{w}^n = \frac{1}{k} (\mathbf{w}^{n+1} - \mathbf{w}^n) \quad \delta_- \mathbf{w}^n = \frac{1}{k} (\mathbf{w}^n - \mathbf{w}^{n-1})$$

and averaging operators approximating the identity as

$$\mu_+ \mathbf{w}^n = \frac{1}{2} (\mathbf{w}^{n+1} + \mathbf{w}^n) \quad \mu_- \mathbf{w}^n = \frac{1}{2} (\mathbf{w}^n + \mathbf{w}^{n-1})$$

Such operations apply analogously if  $\mathbf{w}^n$  is replaced by an interleaved time series  $\mathbf{w}^{n+1/2}$ .

A special operator, which may be associated with trapezoid-rule integration and also approximating a time derivative, may be defined as

$$\delta_\circ = \mu_+^{-1} \delta_+ \quad (17)$$

where  $\mu_+^{-1}$  is interpreted as the operator inverse of  $\mu_+$ . See [19].

#### 4.1 Time-interleaved Scheme

In order to arrive at a fully discrete simulation, one may now introduce time-interleaved sequences  $\mathbf{v}^{n+1/2}$  and  $\mathbf{p}^n$ , representing approximations to  $\mathbf{v}(t)$  and  $\mathbf{p}(t)$  at times  $t = (n + 1/2)k$  and  $t = nk$ , respectively. The sequences are initialised as  $\mathbf{v}^{-1/2} = \mathbf{v}_{-1/2}$  and  $\mathbf{p}^0 = \mathbf{p}_0$ .

A time-interleaved FDTD approximation to the semi-discrete system (10) may then be written directly as

$$\rho \delta_- \mathbf{v}^{n+1/2} + \frac{1}{h} \mathbf{D}_- \mathbf{p}^n = \frac{1}{h} p_\Delta^n \mathbf{J}_v \quad (18a)$$

$$\frac{1}{\rho c^2} \delta_+ \mathbf{p}^n + \frac{1}{h} \mathbf{D}_+ \mathbf{v}^{n+1/2} = \frac{1}{h} v_\Delta^{n+1/2} \mathbf{J}_p \quad (18b)$$

where

$$p_\Delta^n = p_d^n - \mu_- p_c^{n+1/2} \quad v_\Delta^{n+1/2} = v_m^{n+1/2} - \mu_+ v_c^n \quad (19)$$

Here,  $p_d^n$  and  $v_m^{n+1/2}$  are discrete-time external excitation functions (perhaps sampled from  $p_d(t)$  and  $v_m(t)$ , respectively). The time series  $p_c^{n+1/2}$  and  $v_c^n$  are interleaved approximations to  $p_c(t)$  and  $v_c(t)$  respectively. Note the presence of an additional averaging operation  $\mu_+$  applied to the coupling terms in the scheme above.

Using the time domain relationship (3), and approximating time derivatives using  $\delta_\circ$ , as defined in (17), leads to:

$$\sum_{\nu=0}^{D_m} \zeta_{m,\nu} \delta_\circ^\nu v_c^n = Y_0 \sum_{\nu=0}^{M_m} \eta_{m,\nu} \delta_\circ^\nu \mathbf{J}_p^T \mathbf{p}^n \quad (20a)$$

$$\sum_{\nu=0}^{D_d} \zeta_{d,\nu} \delta_\circ^\nu p_c^{n+1/2} = Z_0 \sum_{\nu=0}^{M_d} \eta_{d,\nu} \delta_\circ^\nu \mathbf{J}_v^T \mathbf{v}^{n+1/2} \quad (20b)$$

The system (18), complemented by (19) and (20) constitutes a complete simulation algorithm. As will be shown shortly in Section 4.2, it remains fully explicit, under the standard stability CFL condition for an FDTD scheme.

#### 4.2 Implementation Details

Expanding (18) leads to an update of the form

$$\mathbf{v}^{n+1/2} = \mathbf{v}^{n-1/2} - Y_0 \lambda (\mathbf{D}_- \mathbf{p}^n - \mathbf{J}_v p_d^n) - \frac{Y_0 \lambda}{2} \mathbf{J}_v (p_c^{n+1/2} + p_c^{n-1/2}) \quad (21a)$$

$$\mathbf{p}^{n+1} = \mathbf{p}^n - Z_0 \lambda (\mathbf{D}_+ \mathbf{v}^{n+1/2} - \mathbf{J}_p v_m^{n+1/2}) - \frac{Z_0 \lambda}{2} \mathbf{J}_p (v_c^{n+1} + v_c^n) \quad (21b)$$

where  $\lambda = ck/h$  is the dimensionless Courant number for the scheme.

But, from the expansion of the operators  $\delta_\circ$  appearing in (20), one arrives at

$$p_c^{n+1/2} = Z_0 \gamma_c \mathbf{J}_v^T \mathbf{v}^{n+1/2} + q_c$$

$$v_c^n = Y_0 \beta_c \mathbf{J}_p^T \mathbf{p}^n + r_c$$

where  $\gamma_c$  and  $\beta_c$  are non-negative constants (this follows from the positive realness property of the immittances), and where  $q_c$  and  $r_c$  are collections of previously computed (known) values of  $p_c$ ,  $\mathbf{v}$ ,  $v_c$  and  $\mathbf{p}$ . Using these expressions in the update (21) leads, finally, to the form

$$\underbrace{(\mathbf{I}_v + \alpha_v \alpha_v^T)}_{\Lambda_v} \mathbf{v}^{n+1/2} = \mathbf{b}_v$$

$$\underbrace{(\mathbf{I}_p + \alpha_p \alpha_p^T)}_{\Lambda_p} \mathbf{p}^{n+1} = \mathbf{b}_p$$

where the vectors  $\mathbf{b}_v$  and  $\mathbf{b}_p$  consist of previously computed values of the grid and excitation functions, and where  $\alpha_v$  and  $\alpha_p$  are defined by

$$\alpha_v = \sqrt{\frac{\gamma_c \lambda}{2}} \mathbf{J}_v \quad \alpha_p = \sqrt{\frac{\beta_c \lambda}{2}} \mathbf{J}_p$$

Thus linear system solutions involving the matrices  $\Lambda_v$  and  $\Lambda_p$  as above are required. But, because they are rank one perturbations of the identity, fast  $O(N)$  algorithms are available through the Sherman-Morrison identity [20]:

$$\Lambda_v^{-1} = \mathbf{I}_v - \frac{\alpha_v \alpha_v^T}{1 + \alpha_v^T \alpha_v} \quad \Lambda_p^{-1} = \mathbf{I}_p - \frac{\alpha_p \alpha_p^T}{1 + \alpha_p^T \alpha_p}$$

For sparse definitions of  $\mathbf{J}_p$  and  $\mathbf{J}_v$ , the additional computation to include the source in the FDTD model is  $O(1)$  operations per time step.

#### 4.3 Frequency Domain and Numerical Stability

Under discrete-time Laplace transformation (or  $z$  transformation), a matrix system analogous to (16) results, as a function of a discrete-time frequency variable  $s_d$ , where the unit delay may be interpreted, in the frequency domain, as a multiplicative factor  $z^{-1}$ , where  $z = e^{s_d k}$ . Define the factors

$$s_\pm = \frac{1}{k} (z^{1/2} - z^{-1/2}) \quad s_\circ = \frac{2}{k} \frac{z^{1/2} - z^{-1/2}}{z^{1/2} + z^{-1/2}}$$

and the averaging operator

$$m_\pm = \frac{1}{2} (z^{1/2} + z^{-1/2})$$

corresponding to the difference operators  $\delta_+/\delta_-$ ,  $\delta_\circ$ , and  $\mu_\pm$  accompanied by a half-sample shift. A matrix equation analogous to (14) results:

$$\mathbf{A}(s_d) \mathbf{x} = \mathbf{b}$$

where  $\mathbf{x}$  is the state, as before, and where  $\mathbf{b}$  contains initial conditions and excitation data. Now,  $\mathbf{A}$  is defined by

$$\mathbf{A}(s_d) = \begin{bmatrix} \rho s_\pm \mathbf{I}_v + \frac{Z_0 z_d(s_\circ)}{h} \mathbf{J}_v \mathbf{J}_v^T & -\frac{1}{h} \mathbf{D}_+ \\ \frac{1}{h} \mathbf{D}_+^T & Y_0 y_m(s_\circ) \mathbf{J}_p \mathbf{J}_p^T + \frac{s_\pm}{\rho c^2} \mathbf{I}_p \end{bmatrix}$$

A stability condition follows from the condition that the system matrix  $\mathbf{A}$  possess no zeros for values of the argument  $s_d$  with  $\text{Re}(s) > 0$ . The proof is elaborate, but follows the same reasoning as shown in [19], and we require

$$\lambda = ck/h \leq 1 \quad (22)$$

which is the Courant-Friedrichs-Lewy condition for the 1D wave equation [21]. It is unchanged by the presence of the new source mechanism, due to the use of the difference operator  $\delta_\circ$  in the discretisation of the source dynamics.

#### 4.4 Special Cases

The scheme above includes, as special cases, various source definitions described in the literature. For simplicity, consider the case of  $p_\Delta = 0$ , and where  $y_m = G$  for a constant  $G \geq 0$ . Then (21b) becomes

$$\begin{aligned} \mathbf{p}^{n+1} &= \mathbf{p}^n - Z_0 \lambda \left( \mathbf{D}_+ \mathbf{v}^{n+1/2} - \mathbf{J}_p v_m^{n+1/2} \right) \\ &\quad - \frac{G\lambda}{2} \mathbf{J}_p \mathbf{J}_p^T (\mathbf{p}^{n+1} + \mathbf{p}^n) \end{aligned}$$

When  $G = 0$ , a basic additive (soft) source results. For the case of the hard source, introduce  $p_m^n$  through  $v_m^{n+1/2} = GY_0 (p_m^n + p_m^{n+1})/2$ . Now, one may derive, in the limit as  $G \rightarrow \infty$ ,

$$\mathbf{J}_p^T \mathbf{p}^n = p_m^n \quad (23)$$

and thus the pressure at the excitation point is forced to take on the value of the excitation function  $p_m$ .

## 5. SIMULATION RESULTS

In this section, a variety of simulation results are presented, illustrating the ability of the scheme given in Section 4 to reproduce realistic source excitations, including the interaction of the acoustic field with the source itself. All simulations are run using  $c = 344 \text{ m}\cdot\text{s}^{-1}$ ,  $\rho = 1.2 \text{ kg}\cdot\text{m}^{-3}$ , and over a domain of length  $L = 1 \text{ m}$ , and at a sample rate of 200 kHz. The grid spacing  $h$  is chosen to satisfy the Courant-Friedrichs Lewy condition (22) as close to equality as possible.

### 5.1 Basic Resistive Sources

The most basic form of source model is one for which the source immittances  $y_m = G$  and  $z_d = R$  are positive dimensionless constants. See Figure 1, showing basic results when  $R = G = 1$ , and using sources  $v_m$  and  $p_d$  of the form of a raised cosine of duration 0.2 ms. the resulting pressure field is shown after 1 ms. At top, the symmetric field due to a velocity source is shown, and in the second panel, an asymmetric field due to a pressure source. It is straightforward to generate one-directional sources, through the choices  $p_d = \pm Z_0 v_m$ , when  $R = G$ . Such one-directional propagation is shown in the bottom two panels, with some slight spurious propagation in the opposite direction visible.

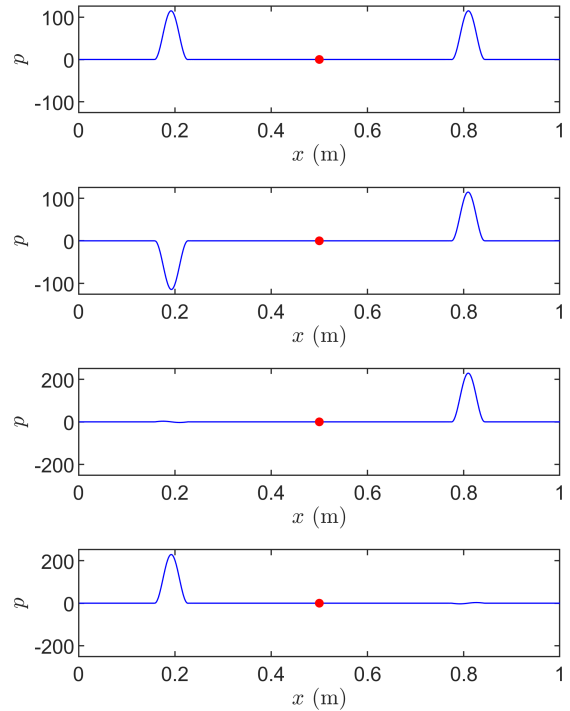


**Figure 1.** Basic resistive sources. Top: using a velocity source  $v_m$ . Second panel: using a pressure source  $p_d$ . Third and fourth panels: one-way sources to the right and left, respectively.

### 5.2 Parallel Source Admittance

Consider now the case of a parallel source admittance  $y_m(s)$ , defined by

$$y_m(s) = \frac{1}{R + Ls + \frac{1}{Cs}} \quad (24)$$

for non-negative constants  $R$ ,  $L$  and  $C$ .

### 5.3 Energy Conservation

Numerical stability for the scheme presented here has been shown using frequency domain concepts, and depends only on the choice of the Courant number and the positive realness property of the source immittances. If one has a concrete realisation of the source immittances, one may go further and directly demonstrate numerical stability of the scheme through the maintenance of an energy balance, relating the rate of change of a discrete numerical energy to losses. In the case of a lossless source immittance, exact numerical energy conservation can be exhibited.

Consider the case above of a traveling wave initial condition only, and with a source characterized by  $z_d = 0$  and  $y_m$  as in (24), with parameters as in the final panel of Figure 2. In Figure 3, the total energy variation is shown, alongside the relative energy variation, showing conservation to machine accuracy as the wave passes through the source location.

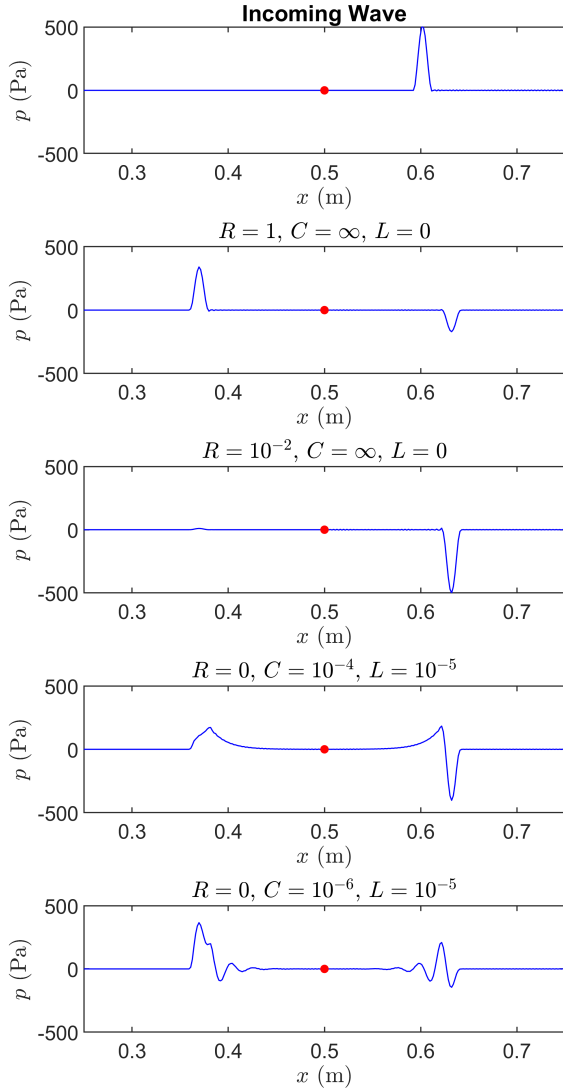


**Figure 2.** Reflections of incoming pressure waves (at top) from a source characterised by a parallel RLC source admittance of the form given in (24), under different choices of  $R$ ,  $L$  and  $C$  as indicated (lower four panels).

## 6. CONCLUDING REMARKS

This paper is intended as a study of a simplified test problem—1D acoustics. It has been shown here that it is possible to associate a complete physical system with various types of numerical source models, and thus reference solutions are available. It remains to be seen whether such an approach may be translated easily to the full 3D setting, in which case the spatial extent of the source term becomes a dominant factor.

Because of the need for simulating the dynamics of the source itself (characterised here by a pair of immittances), new stability concerns emerge, but, using an appropriate

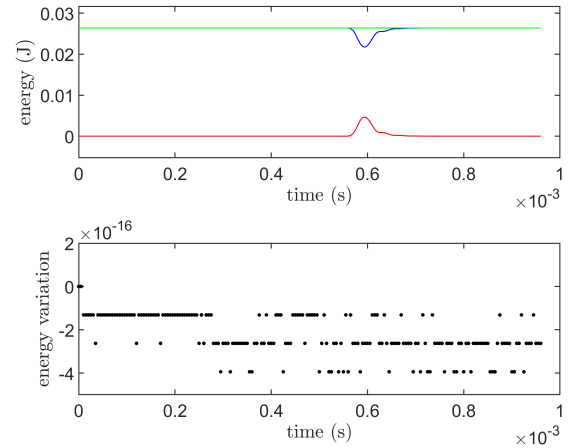


**Figure 3.** Top: total numerical energy, in J, as a function of time (green), energy stored in the acoustic field (blue) and in the source (red). Bottom: normalised energy variation, showing energy conservation to machine accuracy.

discretisation rule for the source dynamics, stability conditions remain unchanged from the case of the simulation of acoustic wave propagation in free space.

## 7. ACKNOWLEDGMENTS

Thanks to Gokul Srinivasan, of the Birla Institute of Technology and Science for many fruitful discussions on this topic.

## 8. REFERENCES

- [1] O. Chiba, T. Kashiwa, H. Shimoda, S. Kagami, and I. Fukai, “Analysis of sound fields in three dimensional space by the time-dependent finite-difference method based on the leap frog algorithm,” *J. Acoust. Soc. Jpn.(J)*, vol. 49, pp. 551–562, 1993.
- [2] D. Botteldooren, “Acoustical finite-difference time-domain simulation in a quasi-cartesian grid,” *J. Acoust. Soc. Am.*, vol. 95, no. 5, pp. 2313–2319, 1994.
- [3] D. Botteldooren, “Finite-difference time-domain simulation of low-frequency room acoustic problems,” *J. Acoust. Soc. Am.*, vol. 98, no. 6, pp. 3302–3308, 1995.
- [4] L. Savioja, T. Rinne, and T. Takala, “Simulation of room acoustics with a 3-D finite-difference mesh,” in *Proc. Int. Comp. Music Conf.*, (Århus, Denmark), pp. 463–466, sep 1994.
- [5] J. Schneider, C. Wagner, and S. Broschat, “Implementation of transparent sources embedded in acoustic finite-difference time domain grids,” *J. Acoust. Soc. Am.*, vol. 136–142, no. 1, pp. 3219–3226, 1998.
- [6] J. Botts, A. Bockman, and N. Xiang, “On the selection and implementation of sources for finite-difference

- methods,” in *Proc. 20th Int. Congr. Acoust.*, (Sydney, Australia), 2010.
- [7] H. Jeong and Y. Lam, “Source implementation to eliminate low-frequency artifacts in finite difference time domain room acoustic simulation,” *J. Acoust. Soc. Am.*, vol. 258–268, no. 1, pp. 1112–1118, 2012.
- [8] D. Murphy, A. Southern, and L. Savioja, “Source excitation strategies for obtaining impulse responses in finite difference time domain room acoustics simulation,” *Appl. Acoust.*, vol. 82, pp. 6–14, 2014.
- [9] A. Pierce, *Acoustics: An introduction to its physical principles and applications*. Acoustical Society of America, 1991.
- [10] S. Bilbao, J. Ahrens, and B. Hamilton, “Incorporating source directivity in wave-based virtual acoustics: Time-domain models and fitting to measured data,” *J. Acoust. Soc. Am.*, vol. 146, no. 4, pp. 2692–2703, 2019.
- [11] J. Sheaffer, M. van Walstijn, and B. Fazenda, “Physical and numerical constraints in source modeling for finite difference simulation of room acoustics,” *J. Acoust. Soc. Am.*, vol. 135, no. 1, 2014.
- [12] C. Peskin, “The immersed boundary method,” *Acta Numerica*, vol. 11, pp. 459–517, 2002.
- [13] R. Mittal and G. Iaccarino, “Immersed boundary methods,” *Annual Review of Fluid Mechanics*, vol. 37, pp. 239–261, 2005.
- [14] X. Sun, Y. Jiang, and X. Jing, “An immersed boundary computational model for acoustic scattering problems with complex geometries,” *J. Acoust. Soc. Am.*, vol. 132, no. 5, pp. 3190–3199, 2012.
- [15] M. van Valkenburg, *Network Analysis*. New York: Dover, 1975.
- [16] L. Weinberg, *Network Analysis and Synthesis*. New York, New York: McGraw-Hill, 1962.
- [17] S. Bilbao, *Numerical Sound Synthesis*. Chichester, UK: John Wiley and Sons, 2009.
- [18] S. Bilbao and B. Hamilton, “Directional sources in wave-based acoustic simulation,” *IEEE Trans. Audio Speech Language Proces.*, vol. 27, pp. 415–428, 2019.
- [19] S. Bilbao and B. Hamilton, “Passive volumetric time domain simulation for room acoustics applications,” *J. Acoust. Soc. Am.*, vol. 145, pp. 2613–2624, 2019.
- [20] J. Sherman and W. Morrison, “Adjustment of an inverse matrix corresponding to a change in one element of a given matrix,” *Annals of Mathematical Statistics*, vol. 21, no. 1, pp. 124–127, 1950.
- [21] R. Courant, K. Friedrichs, and H. Lewy, “On the partial differential equations of mathematical physics,” *Mathematische Annalen*, vol. 100, pp. 32–74, 1928.